

3C1-4

# A Slotted Bow-tie Antenna with Reconfigurable CPW-to-slotline Transition for Pattern Diversity

Sung-Jung Wu and Tzyh-Ghuang Ma<sup>#</sup>

Department of Electrical Engineering, National Taiwan University of Science and Technology, 43, Keelung Rd. Sec.4, Taipei 10607, Taiwan, R.O.C.

Email: [tgma@ee.ntust.edu.tw](mailto:tgma@ee.ntust.edu.tw)

## 1. Introduction

In recent years, reconfigurable antennas have received significant attentions in the field of wireless communications. Such antennas can be used to achieve selectivities in frequencies, polarizations, patterns, as well as antenna gains [1][2]. Pattern reconfigurable antennas are capable of steering antenna radiation patterns to several predetermined directions as so to avoid noise interference or electronic jamming [3][4]. They therefore have the potential benefits of improving data security as well as overall system performance.

In this study, a slotted bow-tie antenna with a new reconfigurable CPW-to-slotline transition is proposed to achieve pattern reconfigurability. By utilizing four PIN diodes, the antenna has the ability to switch radiation patterns alternatively in three different states. The antenna configuration will be discussed in detail in Section 2 along with design concept for reconfigurability. Section 3 then illustrates the simulation and measurement results. Finally, a brief conclusion will be given in Section 4.

## 2. Antenna Configuration and Design Concept

The proposed antenna geometry is shown in Fig. 1(a)(b). The antenna lies in the xy-plane with its normal direction being parallel to the z-axis. This antenna consists of four parts, i.e. a coplanar waveguide (CPW) input, two CPW-to-slotline transitions, a pair of Vivaldi-shaped tapered slots as the radiator, and four PIN diodes for reconfigurability. The proposed antenna was fabricated on a Rogers 4003 substrate with dielectric constant of 3.38 and thickness of 1.6mm. The optimal design parameters are given as follows:  $L_1=25\text{mm}$ ,  $L_2=20\text{mm}$ ,  $L_3=15\text{mm}$ ,  $L_4=19.6\text{mm}$ ,  $L_5=15\text{mm}$ ,  $L_6=19.8\text{mm}$ ,  $L_7=24.8\text{mm}$ ,  $S=3\text{mm}$ ,  $G=0.2\text{mm}$ ,  $W_1=23.3\text{mm}$ ,  $W_2=23.3\text{mm}$ , and  $\alpha=60^\circ$ . To achieve pattern reconfigurability, as shown in Fig. 1(c), two PIN diodes are placed over the input slotline of the slot open of the CPW-to-slotline transition, and the other ones are placed across the slotlines of the CPW input. Depending on the biased states of the diodes, the proposed antenna can be fed by one of the three feeding configurations, which are referred to as the CPW feeding mode, the right-hand slot (RS) feeding mode, and the left-hand slot (LS) feeding mode.

When the antenna is driven by the CPW feeding scheme, the diodes  $D_1$ ,  $D_2$  are turned on whereas  $D_3$ ,  $D_4$  are turned off. In this operation mode, the wave injected into the CPW input line propagates directly down to the radiating slotted bow-tie. The two CPW-to-slotline transitions, on the other hand, are disabled by PIN diodes and have no function. The impedance of the input CPW line is design to be as close to 50 ohm as possible over the band of concern, while the initial slotline impedance of the slotted bow-tie is around 90ohm. As the width of the slotline becomes wider, the impedance becomes larger and larger and hence facilitates the radiations from the tapered slotline to free space with intrinsic impedance 377ohm. It should be emphasized that here the parasitic radiations from the open slot aperture of the transitions are ignored.

For the antenna to be excited by the right-hand slotline, the diodes  $D_1$ ,  $D_3$  are kept forward biased whereas  $D_2$ ,  $D_4$  are reverse biased. Likewise, as the left-hand slotline is used as the feeding input, the diodes  $D_1$ ,  $D_3$  are turned off whereas  $D_2$ ,  $D_4$  are turned on. In either RS or LS feeding

scheme, the wave injected into the CPW input line will propagate into one of the CPW-to-slotline transition upon the diode operation state. The transition is capable of transforming an unbalance CPW mode to a balance slotline mode. As a result, when operating in RS or LS mode, the proposed antenna behaves more like a tapered slot antenna which demonstrates end-fire radiation patterns with good front-to-back ratio. Table I summarizes the diode biased configurations for various antenna feeding schemes.

### 3. Simulation and Measurement Results

Figure 2(a) and (b) compares the simulated and measured return losses of the proposed antenna operated in the CPW and LS feeding modes, respectively. The antenna is well-matched over the frequency band of 4-7 GHz. The simulated return losses are calculated by HFSS 9.2, and reveal good agreement with the measured ones. The discrepancy between the results can be mostly attributed to the interference by the connecting cable, DC biased line, as well as the parasitic effects of PIN diodes. Similar results can be observed in the RS feeding scheme but not shown here for simplicity.

Figure 3 compares the simulated  $yz$ -plane radiation patterns of the proposed antenna in CPW and RS feeding modes at 5GHz. Instead of modeling the PIN diodes as short-circuited pads, here in the simulation the PIN diodes are modeled by constant current source of 20mA to reflect the actual bias condition. As shown in the figure, the radiation pattern in the CPW feeding mode is almost omni-direction whereas the maximum radiation in the RS mode is directed to  $\theta = -90^\circ$  with front-to-back ratio better than 12dB. Similar results can be also observed in the LS feeding scheme but not shown here for the sake of brevity.

The radiation patterns were measured in an anechoic chamber in NTUST. The measured  $yz$ -plane pattern at 5 GHz in the CPW feeding scheme is illustrated in Fig. 4. It reveals excellent agreement with the simulation data in Fig. 3. Figure 5 then compares the measured radiation patterns of the proposed antenna operated in both RS and LS modes at 5 GHz in the  $yz$ -plane. Referring to the figure, the maximum radiation in the RS and LS modes point to  $\theta = -90^\circ$  and  $\theta = 90^\circ$ , respectively, and the front-to-back ratios are both better than 10 dB. The little discrepancy between the simulated and measured results is believed a result of multi-path interference from the connecting cable and SMA connector, etc. The lossless diode model used in the HFSS simulation, on the other hand, accounts for the somewhat gain degradation in the measurement. Finally, it should be noted that although not shown here for simplicity the proposed antenna demonstrates similar pattern reconfigurability in the frequency range of 4 to 6 GHz.

### 4. Conclusion

A novel pattern reconfigurable slotted bow-tie CPW-fed antenna has been presented and discussed. By utilizing four switching PIN diodes on a pair of CPW-to-slotline transitions, the proposed antenna demonstrates pattern reconfigurability in the frequency range of 4 to 6GHz. The simulation results agree well with the measurement ones. This antenna may found applications in various communication systems which are eager for pattern diversity.

### References

- [1] D. Peroulis, K. Sarabandi, L. P. B. Katehi, "Design of Reconfigurable Slot Antenna," *IEEE Trans. Antennas Propagat.*, vol. 53, pp. 645-654, Feb. 2005.
- [2] F. Yang and Y. Rahmat-Samii, "A reconfigurable patch antenna using switchable slots for circular polarization diversity," *IEEE Microw. Wireless Compon. Lett.*, vol. 12, no. 3, pp. 96–98, March 2002.
- [3] C. Jung, M. Lee, G. P. Li, and F. De Flaviis, "Reconfigurable scan-beam single-arm spiral antenna integrated with RF-MEMS switches," *IEEE Trans. Antennas Propagat.*, vol. 54, pp. 455-463, Feb. 2006.

- [4] S. Zhang, G. H. Huff, J. Feng, and J. T. Bernhard, "A pattern reconfigurable microstrip parasitic array," *IEEE Trans. Antennas Propagat.*, vol. 52, pp.2773-2776, Oct. 2004.

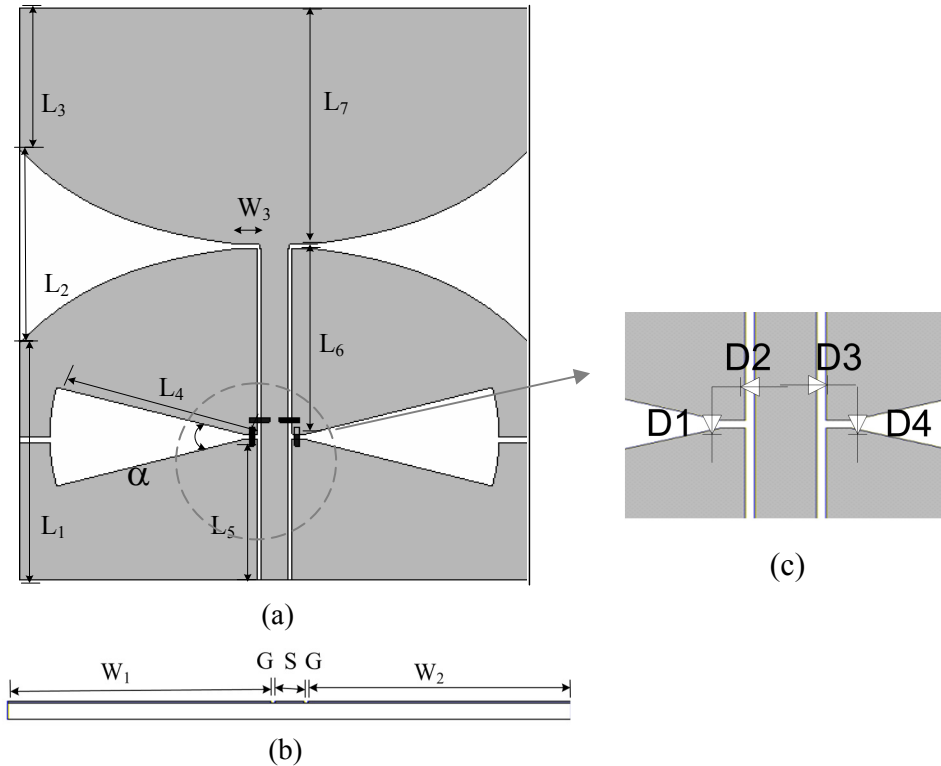


Fig. 1 Geometry of the antenna. (a) Top view. (b) Cross-section view. (c) Diode configuration.

Table1. Pin diodes operating states

Antenna feeding configuration	$D_1$	$D_2$	$D_3$	$D_4$
CPW	On	Off	Off	On
RS	Off	On	Off	On
LS	On	Off	On	Off

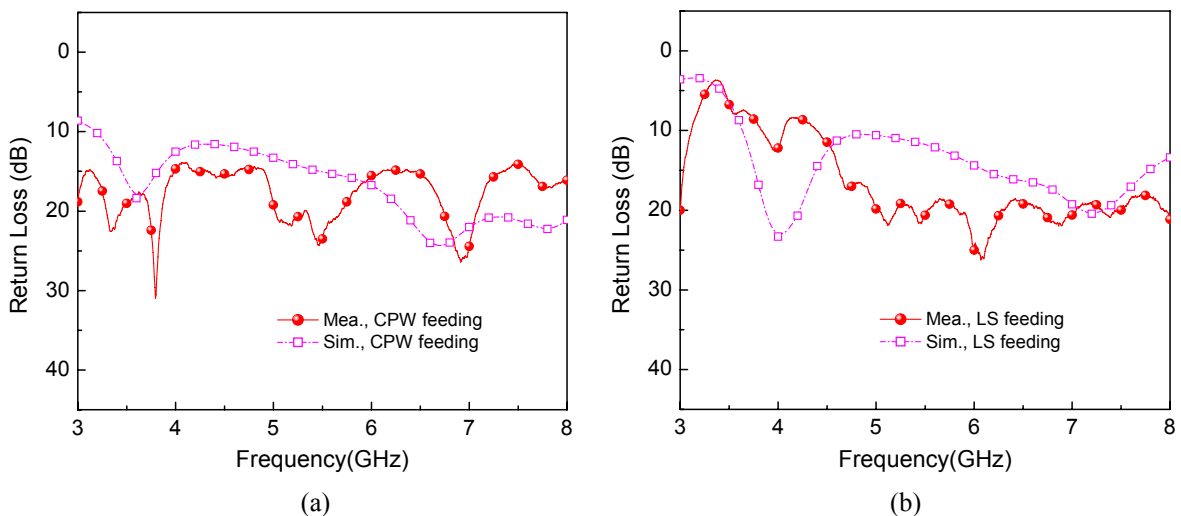


Fig. 2 Simulated and measured return losses (a) CPW feeding. (b) LS feeding.

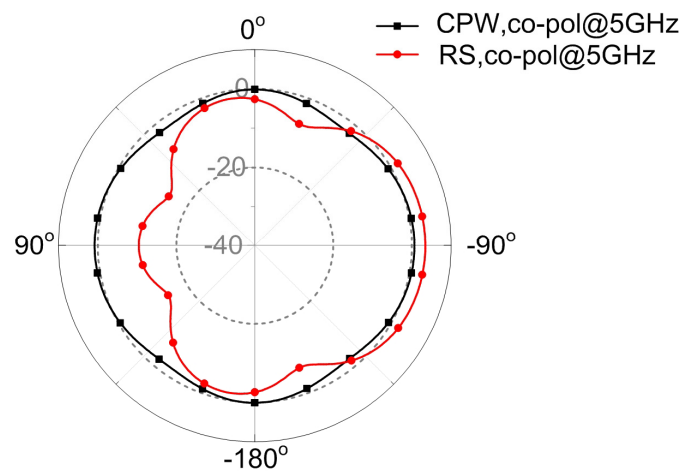


Fig. 3 Simulated radiation patterns in the yz-plane for the CPW and RS feeding schemes

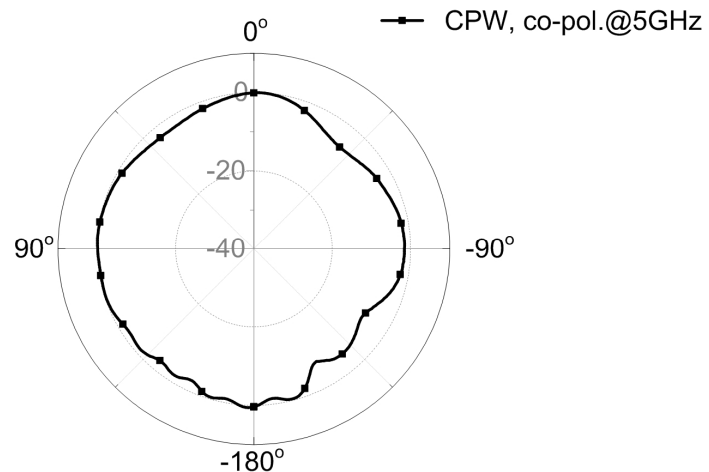


Fig. 4 Measured radiation patterns in the yz-plane for the CPW feeding schemes

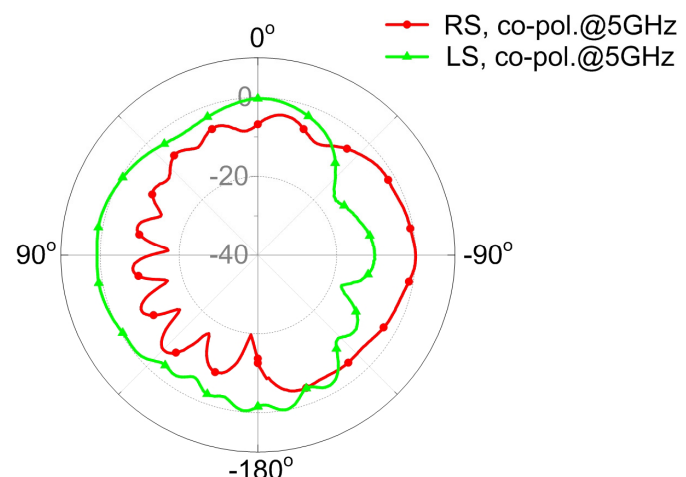


Fig. 5 Measured radiation patterns in the yz-plane for the RS and LS feeding schemes.